Journal of the European Ceramic Society 21 (2001) 1875–1878

www.elsevier.com/locate/jeurceramsoc

Microstructural and electrical characteristics of Y_2O_3-doped $ZnO–Bi_2O_3$-based varistor ceramics

Slavko Bernik [a,*], Srečo Maček [a], Bui Ai [b]

[a] *Jožef Stefan Institute, Jamova 39, Ljubljana, Slovenia*
[b] *Laboratoire de Genie Electrique, Universite Paul Sabatier, Toulouse, France*

Received 4 September 2000; received in revised form 11 October 2000; accepted 15 October 2000

Abstract

The microstructural and electrical characteristics of $ZnO–Bi_2O_3$-based varistor ceramics doped with Y_2O_3 in the range from 0 to 0.9 mol% have been investigated. The addition of Y_2O_3 resulted in the formation of a fine-grained Bi–Zn–Sb–Y–O phase along the grain boundaries of the ZnO grains which inhibits the grain growth. The mean ZnO grain size decreased from 11.3 to 5.4 μm with increasing amounts of Y_2O_3. The threshold voltage (V_T) of the ceramics increased from 150 to 274 V/mm, the non-linear coefficient α was not influenced and remained at approximately 40, and the leakage current also increased with the amount of Y_2O_3 added. On the basis of the Mukae et al. (Mukae, K., Tsuda, K. and Nagasawa, I., Capacitance-vs-voltage characteristics of ZnO varistors. *J. Appl. Phys*., 1979, **50**, 4475–4476) Schottky barrier model of ZnO varistors, the addition of Y_2O_3 resulted in a slight increase in the density of interface states (N_S) and a more pronounced increase in the donor density (N_D), causing a decrease of the barrier height (Φ_B) and the depletion layer width (t). The increase of the leakage current (I_L) with higher amounts of Y_2O_3 added can be ascribed to the increase in donor density (N_D) as well as to the increased amount of Y_2O_3-containing phase at the grain boundaries of ZnO.

Keywords: Electrical properties; Grain size; Microstructure-final; Varistors; ZnO

1. Introduction

ZnO-based varistors are characterised by highly non-linear current-voltage characteristics and a high energy-absorption capability. As a result they are widely used as surge absorbers in electronic circuits, devices and electrical power systems to protect against dangerous over-voltage surges. In the classical ZnO-based varistor, Bi_2O_3 is used as the varistor-former, while other oxides such as Sb_2O_3, Co_3O_4, Mn_3O_4, NiO and others are added in small amounts to further enhance the non-linearity of the varistor's behaviour. The non-linear current-voltage characteristics of ZnO varistor ceramics results from the formation of double Schottky barriers at the grain boundaries. These non-ohmic ZnO–ZnO grain boundaries each have a break-down voltage of 3V and so the overall break-down voltage of the varistor builds up from the non-ohmic grain boundaries between the electrodes of the varistor and can be controlled either by the varistor thickness or the ZnO grain size.[1] High-voltage varistor ceramics require a fine-grained microstructure and Sb_2O_3 is usually added to inhibit the ZnO grain growth.[2,3] Recently it has been reported that the breakdown voltage and energy characteristics of varistor elements can be significantly increased by the introduction of various rare-earth oxides (REO) and Y_2O_3 to the varistor ceramics.[4]

In the present work, the influence of the amount of added Y_2O_3 on the microstructure, current–voltage (I–V) and capacitance–voltage (C–V) characteristics of $ZnO–Bi_2O_3$-based varistor ceramics has been investigated.

2. Experimental

$ZnO–Bi_2O_3$-based varistor samples with the nominal composition (96.2–x) mol% ZnO + 0.9 mol% Bi_2O_3 + 2.9 mol% ($Sb_2O_3 + Co_3O_4 + Mn_3O_4 + NiO + Cr_2O_3$) + xY_2O_3 for $x = 0$, 0.1, 0.3, 0.45 and 0.9 (sample labeled Y0, Y1,

* Corresponding author. Tel.: +386-1-4773-682; fax: +386-1-4263-126.
E-mail address: slavko.bernik@ijs.si (S. Bernik).

0955-2219/01/$ - see front matter
PII: S0955-2219(01)00134-0

Y3, Y5 and Y9, respectively) were prepared by the classical ceramic procedure. Reagent-grade oxides were mixed in proper ratios and homogenized in absolute ethanol using a planetary mill. The powders were dried at 70°C and pressed with 200 MPa into discs 10 mm in diameter and 2 mm thick. The pellets were fired in an alumina crucible at 1230°C for 2 h with heating and cooling rates of 5°C/min in air. Selected samples were also fired at 800 or 900°C for 1 h to determine their phase composition at the onset of sintering.

Densification characteristics were recorded using a heating-stage microscope up to 1300°C at a heating rate 10 K/min. The phase constitution of the samples was analysed by X-ray powder diffraction analysis (XRD). The samples' microstructures were examined using a scanning electron microscope (SEM) in backscattered electron mode. Phase compositions of the samples and the composition of the individual phases were determined by energy-disperse X-ray spectroscopy (EDS) in the SEM. The average ZnO grain size (D) was determined for each sample using 500–800 measurements of grain size per sample. The surface of each grain was measured and its size was calculated as a diameter for circular geometry.

For DC current–voltage (I–V) characterisation, silver electrodes were painted on both surfaces of the disk and fired at 590°C in air. The nominal varistor voltages (V_N) at 1 and 10 mA were measured and the threshold voltage V_T (V/mm) and non-linear coefficient α were determined. The leakage current (I_L) was measured at 0.75 V_N (1 mA).

The C–V characteristics of the varistor samples were measured at room temperature with an LCR meter (Hewlett Packard 4270 A) at a frequency of 10 kHz and a bias voltage in the 0–180V range, controlled by a digital V-meter (Hewlett Packard 3456 A). According to the Schottky-barrier model and its C–V relation, the donor density (N_D), barrier height (Φ_B), density of interface states (N_S) and the depletion-layer width (t) were determined. N_D and Φ_B were determined from the slope and the intercept of the C–V line of the graph $(1/C_B - 1/2C_{B0})^2$ vs. V_G, and N_S, and t were calculated from equations given elsewhere.[5–7]

3. Results and discussion

XRD patterns of the investigated samples are given in Fig. 1. In the sample without Y_2O_3, three phases were identified: the ZnO phase, γ-Bi_2O_3 phase and the $Zn_7Sb_2O_{12}$-type spinel phase. However, in samples doped with Y_2O_3, additional peaks are evident and their intensity increases with increasing amounts of Y_2O_3 in the starting composition. Fig. 2 shows microstructures of the investigated samples. As can be seen from these back-scattered SEM micrographs, the three phases

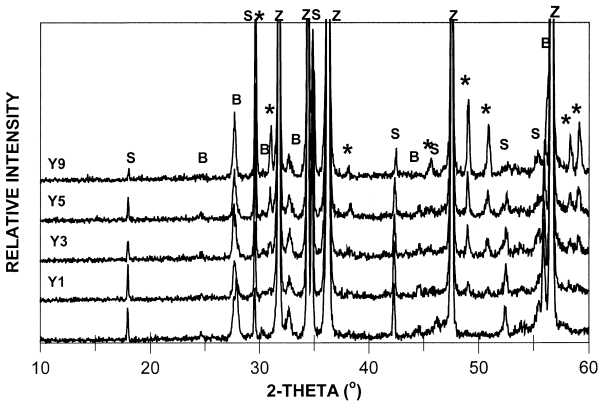

Fig. 1. XRD patterns of ZnO–Bi_2O_3-based varistor ceramics doped with Y_2O_3 and fired at 1230°C for 2 h; (a) Y0 (0 mol%), (b) Y1 (0.1 mol%), (c) Y3 (0.3 mol%), (d) Y5 (0.45 mol%) and (e) Y9 (0.9 mol%). Z: ZnO phase, B: γ-Bi_2O_3 phase, S: $Zn_7Sb_2O_{12}$-type spinel phase, *: Y_2O_3-containing phase.

already identified by XRD analysis were observed in sample without Y_2O_3, while in samples doped with Y_2O_3 an additional phase was detected. EDS analysis revealed this to be a Bi–Zn–Sb–Y–O phase with traces of oxides of Cr, Mn, Co and Ni. Determination of the exact composition by EDS analysis is difficult due to the small grains of Y_2O_3-containing phase which have a size below 2 μm. However, in all the samples a cation ratio of Bi:Zn:Sb:Y:O close to 0.4:1:1:1 was determined for the Y_2O_3-containing phase. Y_2O_3 was not detected in the ZnO phase nor in Bi_2O_3-rich and $Zn_7Sb_2O_{12}$-type spinel secondary phases above the detection limit for EDS analysis, which is at roughly 0.1 wt.%. Formation of the Y_2O_3-containing phase was already observed at lower temperatures. In samples fired at 800°C, a Bi–Zn–Y–O phase was identified by EDS analysis in addition to the ZnO phase and the $Zn_7Sb_2O_{12}$-type spinel phase in the fine-grained microstructure of the Y_2O_3-doped samples. After firing at 900°C, the Bi–Zn–Sb–Y–O-type phase is already present with the Bi_2O_3-rich and $Zn_7Sb_2O_{12}$-type spinel secondary phases. The Bi_2O_3-rich phase melts at 740°C and in samples fired at 900°C the presence of a liquid phase resulted in a significantly coarser ZnO grain size in comparison with the Y_2O_3-doped samples fired at 800°C. In the sample without Y_2O_3 (Y0), the Bi_2O_3-rich phase is present in addition to the $Zn_7Sb_2O_{12}$-type spinel and $Bi_3Zn_2Sb_3O_{11}$-type pyrochlore secondary phases at 800°C. The Y_2O_3-containing phase bounds the Bi_2O_3 and influences the sintering of the samples. In samples with a higher amount of Y_2O_3 in the starting composition the onset of sintering is shifted to a higher temperature, as can be seen from the densification curves in Fig. 3.

The amount of Y_2O_3-containing phase increased with the amount of Y_2O_3 in the starting composition. It is fine grained with a grain size significantly smaller than the $Zn_7Sb_2O_{12}$-type spinel phase, distributed uniformly

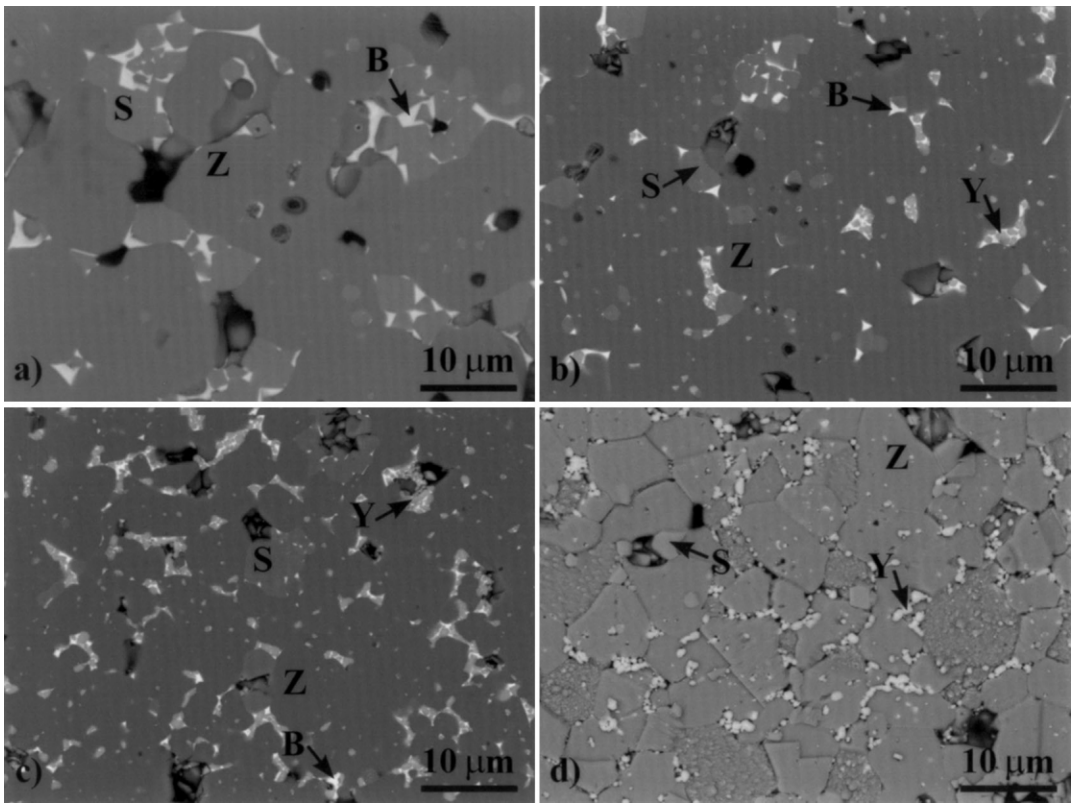

Fig. 2. Microstructures of ZnO–Bi_2O_3 based varistor ceramics fired at 1230°C for 2 h, doped with varying amounts of Y_2O_3; (a) 0 mol% (Y0), (b) 0.3 mol% (Y3), (c) 0.9 mol% (Y) and (d) 0.9 mol% (Y9 — microstructure etched with diluted hydrochloric acid). Z: ZnO phase, B: Bi_2O_3-rich phase, S: $Zn_7Sb_2O_{12}$-type spinel phase, Y: Y_2O_3-containing phase.

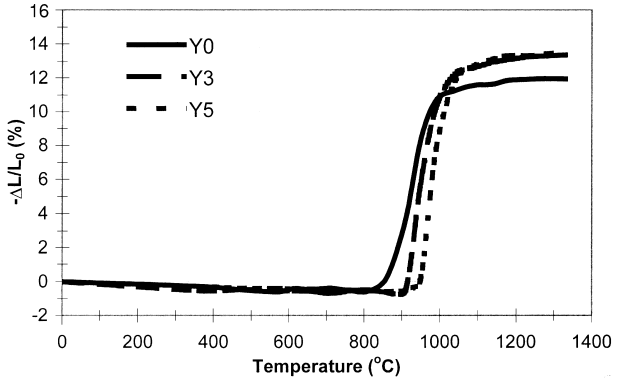

Fig. 3. Densification curves of ZnO–Bi_2O_3 based varistor samples doped with varying amounts of Y_2O_3.

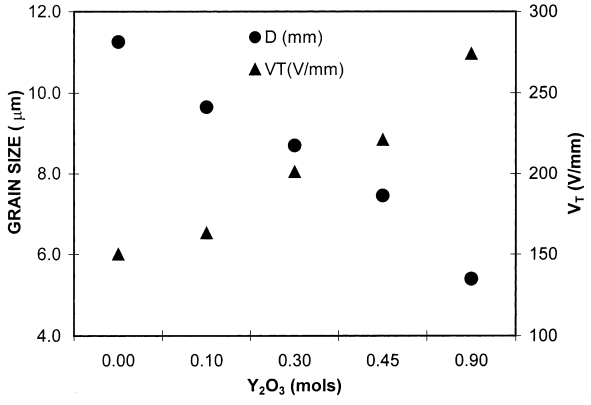

Fig. 4. ZnO grain size D (μm) and threshold voltage V_T (V/mm) vs. amount of Y_2O_3 added to the ZnO–Bi_2O_3-based varistor ceramics fired at 1230°C for 2 h.

along the grain boundaries of the ZnO (Fig. 2d) and may inhibit grain growth effectively. The size of ZnO grains uniformly decreased with the amount of Y_2O_3 added. This resulted in a significant increase in the threshold voltage (V_T) of the varistor ceramics and is also shown in Fig. 4. Doping with Y_2O_3 did not influence the non-linear coefficient α, which was approximately 40 (± 3) for all the investigated samples. However, the leakage current (I_L) of the samples increased with increasing amounts of Y_2O_3 (Table 1). The increase is particularly significant in the sample with the largest addition of Y_2O_3 (0.9 mol%). It can be assumed that such an increase of leakage current in this sample is at least to some extent related to a pronounced increase in the amount of Y_2O_3-containing phase at the grain boundaries of ZnO. The electrical characteristics (resistivity) of this Bi–Zn–Sb–Y–O (Cr, Co, Mn, Ni) phase, however, are not known at present. It should also be

Table 1
C–V characteristic parameters of ZnO–Bi_2O_3-based varistor ceramics doped with Y_2O_3 and leakage current I_L at 0.75 V_N (1 mA)

Y_2O_3 (mol)	N_D ($\times 10^{18}$ cm^{-3})	N_S ($\times 10^{12}$ cm^{-2})	Φ_B (eV)	t (nm)	I_L ($\times 10^{-3}$ A)
0	0.79	2.88	1.12	37	0.04
0.1	1.17	3.00	0.82	26	0.05
0.3	0.70	2.34	0.83	33	0.07
0.45	1.22	2.90	0.74	24	0.11
0.9	1.91	3.61	0.73	19	0.89

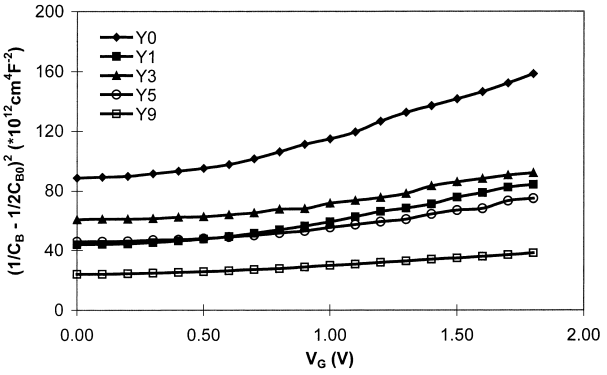

Fig. 5. C–V characteristics of ZnO–Bi_2O_3-based varistor ceramics doped with Y_2O_3 in the range from 0 to 0.9 mol%; C_B: capacitance per unit area of a grain boundary, C_{BO}: value of C_B when $V_G = 0$, V_G: applied voltage per grain boundary.

considered that this phase influences the distribution of all other varistor dopants along the grain boundaries of ZnO as well.

The capacitance–voltage (C–V) characteristics of the investigated samples are shown in Fig. 5 and the characteristic C–V parameters, using the Mukae et al. analysis,[5] are given in Table 1. On the basis of this analysis, doping with Y_2O_3 resulted in an increase of the donor density (N_D) as well as the density of interface states (N_S). Generally, the barrier height (Φ_B) increases with an increase of the density of interface states, however, a larger variation rate of donor concentration prevailed and the barrier height (Φ_B) decreased with larger amounts of Y_2O_3. The depletion-layer width was observed to decrease as well. An increase in the donor concentration can also contribute to an increase in the leakage current, and this is particularly significant in the sample with 0.9 mol% of Y_2O_3.

4. Conclusions

Doping of ZnO–Bi_2O_3-based varistor ceramics with Y_2O_3 results in the formation of a Bi–Zn–Sb–Y–O phase with a cation ratio close to 0.4:1:1:1. Y_2O_3 does not enter the ZnO grains and was not detected in either the Bi_2O_3-rich phase or the $Zn_7Sb_2O_{12}$-type spinel phase. In samples with higher amounts of Y_2O_3 in the starting composition and hence a higher amount of Y_2O_3-containing phase which bounds the Bi_2O_3, the onset of sintering is shifted to a higher temperature. The fine-grained Y_2O_3-containing phase present at the grain boundaries strongly inhibits ZnO grain growth. The ZnO grain size decreased from 11.3 to 5.4 μm with increasing amounts of Y_2O_3. The decrease in the ZnO grain size resulted in an increase in the threshold voltage (V_T) of the samples from 150 to 274 V/mm. Doping with Y_2O_3 does not influence the non-linear coefficient α of the varistor ceramics while the leakage current (I_L) increases with increasing amounts of Y_2O_3.

Schottkey barrier analysis of C–V data showed that Y_2O_3 doping results in an increase in the density of interface states (N_S) and an even greater rise in the donor density (N_D). The barrier height (Φ_B) decreases with increasing amounts of Y_2O_3, from 1.12 eV in the Y_2O_3-free sample to 0.78 ± 0.05 eV for the Y_2O_3-doped samples.

Acknowledgements

The work has been carried out as part of the PROTEUS project for Slovene–French scientific and technical collaboration. The financial support of the Ministry of Science and Technology of Slovenia and EDIGE is gratefully acknowledged.

References

1. Clarke, D. R., Varistor ceramics. *J. Am. Ceram. Soc.*, 1999, **82**, 485–502.
2. Asokan, T. G., Iyengar, N. K. and Nagabhushana, G. R., Studies on microstructure and density of sintered ZnO-based non-linear resistors. *J. Mater. Sci.*, 1987, **22**, 2229–2236.
3. Kim, J., Kimura, T. and Yamaguchi, T., Microstructure development in Sb_2O_3-doped ZnO. *J. Mater. Sci.*, 1989, **24**, 2581–2586.
4. Shichimiya, S., Yamaguchi, M., Furuse, N., Kobayashi, M. and Ishibe, S., Development of advanced arresters for GIS with new zinc-oxide elements. *IEEE Trans. Power Delivery*, 1998, **13**, 465–471.
5. Mukae, K., Tsuda, K. and Nagasawa, I., Capacitance-vs-voltage characteristics of ZnO varistors. *J. Appl. Phys.*, 1979, **50**, 4475–4476.
6. Fan, J. and Freer, R., The electrical properties and d.c. degradation characteristics of silver doped ZnO varistors. *J. Mater. Sci.*, 1993, **28**, 1391–1395.
7. Sun, H. T., Zhang, L. Y. and Yao, X., Electrical nonuniformity of grain boundaries within ZnO varistors. *J. Am. Ceram. Soc.*, 1993, **76**, 1150–1155.